IN VITRO METABOLISM OF THE MAMMALIAN SOLUBLE EPOXIDE HYDROLASE INHIBITOR, 1-CYCLOHEXYL-3-DODECYL-UREA

TAKAHO WATANABE, CHRISTOPHE MORISSEAU, JOHN W. NEWMAN, AND BRUCE D. HAMMOCK

Department of Entomology and Cancer Research Center, University of California, Davis, California

This article is available online at http://dmd.aspetjournals.org

ABSTRACT:

The metabolism of the soluble epoxide hydrolase (sEH) inhibitor, 1-cyclohexyl-3-dodecyl-urea (CDU), was studied in rat and human hepatic microsomes. The microsomal metabolism of CDU enhanced sEH inhibition potency of the reaction mixture and resulted in the formation of several metabolites. During the course of this study, a sensitive and specific high-performance liquid chromatography with tandem mass spectrometry analytical method was developed to investigate simultaneously the production of these metabolites. In both rat and human hepatic microsomes, CDU was ultimately transformed into the corresponding ω-carboxylate; however, the rodent tissue appeared to perform this transformation more rapidly. After a 60-min incubation in rat hepatic microsomes, the percentage of residual CDU, the ω-carboxylate, and the intermediary ω-hydroxyl were about 20%, 20%, and 50%, respectively. Carbon monooxide inhibited the metabolism of CDU by rat hepatic microsomes, suggesting that the initial step is catalyzed by cytochrome P450. Further metabolism was enhanced by the addition of NAD, suggesting that dehydrogenases are associated with intermediate metabolic steps. Regardless, the ultimate product of microsomal metabolism, 12-(3-cyclohexyl-ureido)-dodecanoic acid, is also an excellent sEH inhibitor with several hundred-fold higher solubility, supporting the hypothesis that CDU has prodrug characteristics. These findings will facilitate the rational design and optimization of sEH inhibitors with better physical properties and improved metabolic stability.

Epoxide hydrolases (EH[1]; EC 3.3.2.3) are enzymes that add water to epoxides (Oesch, 1973). These enzymes are widely distributed throughout the animal and plant kingdoms and not only metabolize epoxides of drugs and xenobiotics, but also catalyze the hydration of endogenous compounds. In mammals, the microsomal EH and soluble EH (sEH), which detoxify mutagenic, carcinogenic, and xenobiotic epoxides (Wixtrom et al., 1985), have broad and complementary substrate selectivities (Hammock et al., 1997). The sEH rapidly hydrates fatty acid epoxides (Gill and Hammock, 1979) and seems especially involved in the metabolism of epoxides of arachidonic acid (Chacos et al., 1983; Halarnkar et al., 1989; Zeldin et al., 1995) and linoleic acid (Moghaddam et al., 1997; Zheng et al., 2001). Epoxides of arachidonic acid (epoxyeicosatrienoic acids) are endogenous regulators (Capdevila et al., 2000) that influence blood pressure by modulating cardiac output, vascular resistance, renal fluid, and electrolyte balance, whereas the diols of linoleate epoxides have been implicated in inflammatory disorders, such as acute respiratory distress syndrome (Moghaddam et al., 1997), and may be endogenous regulators of vascular permeability and inflammation (Slim et al., 2001). Therefore, the modulation of endogenous lipid epoxides using sEH inhibitors may have therapeutic benefits in both hypertensive and inflammatory conditions.

The development of potent and stable inhibitors of sEH has facilitated the inhibition of this enzyme in both in vitro and in vivo models (Morisseau et al., 1999; Yu et al., 2000; Fang et al., 2001). Oral availability is also an important factor for long-term in vivo studies. However, the poor solubility and relatively short duration of action limits the use of the most potent urea-based sEH inhibitors reported to date. We have reported that some of our potent inhibitors are metabolized very quickly in hepatic microsomes (Watanabe and Hammock, 2001). Although the low inhibitor solubility can be understood by log P calculations, the absorption, distribution, metabolism, and excretion properties of these chemicals most likely account for their short time of action. Therefore, understanding the route of metabolism should provide information leading to the design of more stable inhibitors. In addition, we hypothesize that metabolic transformations of the aliphatic ω-terminal of one class of inhibitory lead compounds will not alter their inhibition potency but, rather, will enhance their water solubility. To test this hypothesis, we have focused the current study on the metabolism of 1-cyclohexyl-3-dodecyl-urea (CDU), one potent inhibitor of sEH (Morisseau et al., 2002). To assess the metabolism of these compounds, a specific and sensitive analytical method is required. High-performance liquid chromatography with tandem mass spectrometry (LC/MS-MS) provides a useful tool for drug metabolism

[1] Abbreviations used are: EH, epoxide hydrolase(s); sEH, soluble epoxide hydrolase; CDU, 1-cyclohexyl-3-dodecyl-urea; LC/MS-MS, high-performance liquid chromatography with tandem mass spectrometry; CUDA, (12-(3-cyclohexyl-ureido)-dodecanoic acid; CTU, 1-cyclohexyl-3–tetradecyl-urea; CHDU, 1-cyclohexyl-3-(12-hydroxy-dodecyl)-urea; CODU, 1-cyclohexyl-3-(12-oxo-dodecyl)-urea; P450, cytochrome P450; ABT, aminobenzotriazol; ESI, electrospray ionization; HPLC, high-performance liquid chromatography; MRM, multiple reaction monitoring.

Address correspondence to: Bruce D. Hammock, Department of Entomology & Cancer Research Center, University of California, Davis, CA 95616. E-mail: bdhammock@ucdavis.edu

studies. Here we report the development of a LC/MS-MS-based method for the simultaneous determination of CDU and its major metabolites, and the use of this method to investigate the microsomal metabolism of this sEH inhibitor. The obtained results are used to propose refinements in the optimal structure of sEH inhibitors for in vivo applications.

Materials and Methods

Chemicals. CDU, 12-(3-cyclohexyl-ureido)-dodecanoic acid (CUDA), and 1-cyclohexyl-3-tetradecyl-urea (CTU; internal standard) were synthesized in our laboratory. These products were purified by recrystallization and characterized structurally by ^1H and/or ^{13}C NMR, infrared, and mass spectroscopy as previously described (Morisseau et al., 2002). β-Nicotinamide adenine dinucleotide phosphate sodium salt (NADP), β-nicotinamide adenine dinucleotide (NAD), glucose-6-phosphate dehydrogenase, D-glucose 6-phosphate monosodium salt, and aminobenzotriazole were obtained from Sigma-Aldrich (St. Louis, MO), and anhydrous magnesium chloride was from Aldrich Chemical Co. (Milwaukee, WI). HPLC-grade methanol, acetonitrile, and ethyl acetate, reagent-grade monobasic monohydrate sodium phosphate, anhydrous dibasic sodium phosphate, and formic acid (88%) were purchased from Fisher Scientific (Pittsburgh, PA). Water (>18.0 MΩ) used was purified by the NANO pure II system (Barnstead, Newton, MA).

LC/MS-MS. The LC/MS-MS experiments were carried out using a Micromass Quattro Ultima triple quadrupole tandem mass spectrometer (Micromass, Manchester, UK) equipped with atmospheric pressure ionization source [atmospheric z-spray pressure chemical ionization or electrospray ionization (ESI) interface]. The HPLC system consisted of a Waters model 2790 separations module (Waters, Milford, MA) equipped with a Waters model 2487 dual λ absorbance detector. The mass spectrometer was coupled to the outlet of the HPLC column or syringe pump for optimization with PEEK tubing. Data were manipulated with MassLynx software (Ver. 3.5).

An XTerra MS C_{18} column (30 × 2.1 mm i.d., 3.5 μm; Waters) was used with a flow rate of 0.3 ml/min at ambient temperature. Solvents A and B were 0.1% formic acid and acetonitrile containing 0.1% formic acid, respectively. Solvents were degassed by vacuum. Mobile phases were mixed with a linear gradient from 40% B to 100% B over 0 to 5 min, and then isocratic for 8 min with 100% B. The post-run was carried out to equilibrate the column to the initial conditions for 1 min before the next run. Five microliters of standard and the extracted microsome samples were injected onto the column.

The ESI was performed in the positive ion mode with a capillary voltage at 1.0 kV. The source and the desolvation temperature were set at 100°C and 300°C, respectively. Cone gas (N_2) and desolvation gas (N_2) were maintained at flow rates of 130 and 630 l/h, respectively. The optimum cone voltages were set at 80 V for CDU, 80 to 85 V for metabolites, and 100 V for CTU (internal standard), respectively. Mass spectra of the precursor ions were obtained by syringe pump infusions, while scanning over the range of 50 to 350 m/z at 3 s/scan. Data were acquired in the multichannel analysis mode and continuum mode. Quantitative analysis was performed in the multiple reaction monitoring (MRM) mode with a dwell time of 0.6 s. Ultra pure argon (99.9999%) was used as a collision gas at a pressure of 2.5 milli-torr for collision-induced dissociation.

Sample Preparation. CDU, CUDA, and CTU solutions (50–200 μg/ml) were prepared as stock solutions by dissolving the pure compounds in methanol. Standard solutions were stored at 4°C in the dark before use. Standard solutions (1 μg/ml) were prepared for MS optimization study. The concentration range in the calibration studies varied from 2 to 500 ng/ml. A stock solution of CTU for use as an internal standard was prepared in methanol and diluted to a concentration of 500 ng/ml with methanol.

Microsomal Incubation. Ten male Fisher 344 rats (8 weeks old; Charles River Laboratories, Inc., Wilmington, MA) and 5 male Fisher 344 rats (8 weeks old; Charles River) treated with 1.5 mmol/kg clofibrate were used for the preparation of pooled liver microsomes (Guengerich, 1982). Protein concentration and ω-hydroxylation of lauric acid were determined by the Bradford method (Bradford, 1976) and a radiometric method with [^{14}C]lauric acid as substrate (Orton and Parker, 1982). A pooled male human liver ($n = 10$) microsome preparation (Gentest, Woburn, MA) was also used to evaluate CDU metabolism, allowing a comparison with rodent data.

For CDU metabolism studies, 0.05 mg of liver microsomal protein (890 μl) were brought to a final volume of 1 ml in 100 mM sodium phosphate buffer at pH 7.4. This protein was preincubated for 5 min in open glass tubes immersed in a shaking bath at a constant temperature of 37°C. After this preincubation, 10 μl of a 100 μM solution of CDU in methanol was added, and the reaction was initiated by the addition of 100 μl of the NADPH generating system. The NADPH regenerating system consisted of 2 mM NADP, 57 mM glucose 6-phosphate, 3.5 units/ml glucose-6-phosphate dehydrogenase, and 50 mM magnesium chloride dissolved in 100 mM sodium phosphate buffer at pH 7.4. Each incubation mixture (1 ml total volume) was incubated in a shaking water bath kept at 37°C for 5, 10, 20, 30, 40, or 60 min. A control was prepared by the addition of 1 ml of ethyl acetate after adding the NADPH generating system. Reactions were terminated by the addition of 1 ml of cold ethyl acetate, and kept in ice water until isolation. A 200-μl aliquot of 500 ng/ml CTU was added to the samples. The samples were then vortexed and centrifuged at 6000 rpm (4000 g) for 5 min. The aqueous phases were extracted twice with ethyl acetate, extracts were combined and dried under nitrogen. The residue was reconstituted in 1 ml of methanol. Aliquots (5 μl) were injected onto the LC-MS-MS system.

To investigate the metabolic pathways involved in CDU transformation, cofactors, inhibitors, and microsomes from either clofibrate-fed or control rats were selectively employed. Specifically, NADPH and carbon monoxide were used to evaluate P450 metabolism, while NAD was used as a dehydrogenase cofactor. Clofibric acid is a known inducer of CYP4A and β-oxidation (Gibson et al., 1982). Moreover, ABT was used to inhibit CYP4A. After a 10-min incubation of CDU with microsomes and the NADPH generating system, carbon monooxide gas was bubbled in the mixture to inhibit NADPH-dependent P450 metabolism. Samples were incubated for an additional 50 min, followed by extraction and LC/MS-MS analysis as described above. Finally 600 μl of additional microsomes and 100 μl of 2 mM NAD were added to 300-μl aliquots of microsomes after 40 min of incubation; then, microsomes were incubated for 40 min at 37°C. After termination by the addition of ethyl acetate, metabolites in microsomes were also analyzed by LC/-MS-MS.

sEH Activity Assay. Dissociation constants were determined by following the method described by Dixon (1972) for competitive tight-binding inhibitors, using [^3H]1,3-diphenyl-*trans*-propene oxide as substrate (Borhan et al., 1995). Inhibitors at concentrations between 10 and 100 nM were incubated in triplicate for 5 min in sodium phosphate buffer, pH 7.4, at 30°C with the recombinant enzyme (2 nM sEH) (Grant et al., 1993). Substrate ($10 \leq$ [S]$_{final} \leq 50$ μM) then was added. Velocity was measured as described (Borhan et al., 1995).

Log P Measurement. CDU or CUDA (10 mg) was added to 4 ml of 1-octanol in a 10-ml glass centrifuge tube, and samples were sonicated for 5 min. Four milliliters of 100 mM phosphate buffer (pH 7.4) then was added to the sample solutions. Then sample solutions were incubated in a shaking bath at 37°C for 24 h. After centrifugation at 6000 rpm for 5 min, 1 ml of the water layer was used for further extraction. Two hundred microliters of 500 ng/ml CTU was added to the samples, and samples were extracted twice with 800 μl of ethyl acetate. Extracts were combined and dried under nitrogen. The residue was reconstituted in 1 ml of methanol. Aliquots (5 μl) were injected onto the LC/MS-MS system.

Kinetics of Metabolism. Linear conditions for the formation of hydroxylate metabolite were evaluated regarding protein content and incubation time for rat hepatic microsomes. The optimum conditions for the kinetics study were 0.05 mg/ml protein concentration of microsomes at 37°C for a 2-min incubation. A substrate concentration range of 100 to 3000 nM was used for the kinetic study. Kinetic data (K_m and V_{max}) were analyzed by Michaelis-Menten and Hanes-Woolf plots. The intrinsic clearance was calculated using the following equation: v $Cl_{int} = Vmax/Km$.

Statistical Analysis. Analysis of statistical significance, where appropriate, was performed using Student's t test.

Results

Identification of CDU Metabolites in Rat Hepatic Microsomes. To elucidate CDU metabolism, CDU was incubated in rat hepatic microsomes with a NADPH generating system for 60 min. After extraction with ethyl acetate, the sample was analyzed by positive mode ESI LC/MS-MS, collecting a full scan (m/z 50–400). Residual

CDU (20%) and several novel chromatographic peaks were found when compared with control samples (data not shown). To identify the unknown peaks, daughter ion scans were performed (Fig. 1). The three dominant metabolites of CDU identified in rat hepatic microsomes were the hydroxylic [1-cyclohexyl-3-(12-hydroxy-dodecyl)-urea] (CHDU), aldehydic [1-cyclohexy-3-(12-oxo-dodecyl)-urea] (CODU), and carboxylic (CUDA) metabolites.

Analysis Optimizations for CDU and Its Metabolites. The metabolism of CDU in rat hepatic microsomes was investigated using tandem mass spectrometry with a 13-min HPLC solvent gradient. CDU was efficiently ionized in the positive mode due to the presence of nitrogens in the structure. To optimize ionization and fragmentation conditions, 1 μg/ml CDU was delivered into the mass spectrometer using a syringe pump with a 10 μl/min flow rate. The protonated molecule m/z 311 (parent ion) $[M + H]^+$ was the most abundant ion, and the acetonitrile adduct ion was also observed in the Q1 scan spectrum with ESI. For MS-MS experiments, samples were separated chromatographically, and protonated ions for each of the analytes were found as follows: CDU, m/z 311; CHDU, m/z 327; CODU, m/z 325; and CUDA, m/z 341, as shown in Table 1. The ESI tandem mass product ion spectra resulting from collision-induced dissociation of each molecular ion are depicted in Fig. 1. As expected, similarities in the fragment patterns (N-C bond cleavage) were observed for all analytes. As shown in Table 1, the most abundant product ions were m/z 229 (CDU), m/z 202 (CHDU), m/z 200 (CODU), m/z 198 (CUDA), and m/z 257 (CTU; internal standard), respectively. Therefore, these product ions were used for the MRM scan. To optimize MS-MS conditions, the collision voltages between 10 and 32 eV were evaluated. Considering sensitivity, background, and characterization of analyte, optimum collision voltages were set for each target (Table 1).

Chromatographic resolution of the CDU metabolites was accomplished with a 30-mm reversed phase semi-micro HPLC column and a linear solvent gradient. A total ion chromatogram and MRM profiles of CDU and its metabolites using the described ESI LC/MS-MS conditions are shown in Fig. 2. Although baseline resolution of CUDA, CHDU, and CODU was not achieved, the specific detection of each analyte was accomplished using MRM scans. Good linearities were observed for CDU and CUDA between the concentration and the response corresponding to the peak area ratios in the concentration range from 2 to 400 ng/ml ($r \geq 0.999$). The concentration of CODU and CHDU was estimated using the relative response factor of CUDA.

The extraction efficiencies for each analytical target were then evaluated. When 50 to 250 ng/ml CDU was spiked into rat hepatic microsomes, extraction recoveries were 101.9 ± 5.9 to $107.7 \pm 4.6\%$. Extraction recovery of CUDA was $88.0 \pm 5.0\%$. Since CHDU and CODU polarities are intermediate to that of CDU and CUDA, we assume that the extraction efficiencies for these primary metabolites are at least equal to that of CUDA.

Hepatic Microsomal Metabolism of CDU. The time-dependent formation of CDU metabolites in rat and human hepatic microsomes are shown in Fig. 3. When 1 μM CDU was incubated in rat microsomes at 37°C for 1 h, 70% of the CDU was metabolized within 10 min of incubation. On the other hand, over 90% of the CUDA in a 1 μM solution remained after 1 h of incubation with rat microsomes (data not shown). After 10 min of incubation, 312 ng/ml CDU was transformed into 90, 163, 36, and 17 ng/ml CDU, CHDU, CODU, and CUDA (accounting for ~95% of the initial mass), respectively. The concentration of CHDU decreased slightly after 10 min, and the concentrations of CODU and CUDA gradually increased until 60 min. To measure the in vitro metabolic rate, the kinetics of the NADPH-dependent metabolism of 100 to 3000 nM CDU to CHDU was examined with rat hepatic microsomes. The calculated kinetics parameters of $K_{m\ app}$ and $V_{max\ app}$ were 223 nM and 1667 pmol/min/mg protein, respectively, by Hanes-Woolf plot and Michaelis-Menten plot. The intrinsic clearance, calculated as V_{max}/K_m, was 7.47 ml/min/mg for CHDU. Although the relative rate of CHDU formation in human and rat microsomes was similar (Fig. 3), the CODU and CUDA formation was significantly lower in the human tissue preparation.

Microsomal Metabolism Increased sEH Inhibitor Potency. Incubating CDU with microsomes and NADPH for 10 min increased the sEH inhibition potency of the reaction mixture by ~10% (Fig. 4A). Similarly, the sEH inhibition potency of solutions containing between 10 and 100 nM CDU were increased when incubated for 30 min with microsomes (Fig. 4B). On the other hand, sEH inhibition by CUDA was not influenced by either addition of microsomes or incubation time.
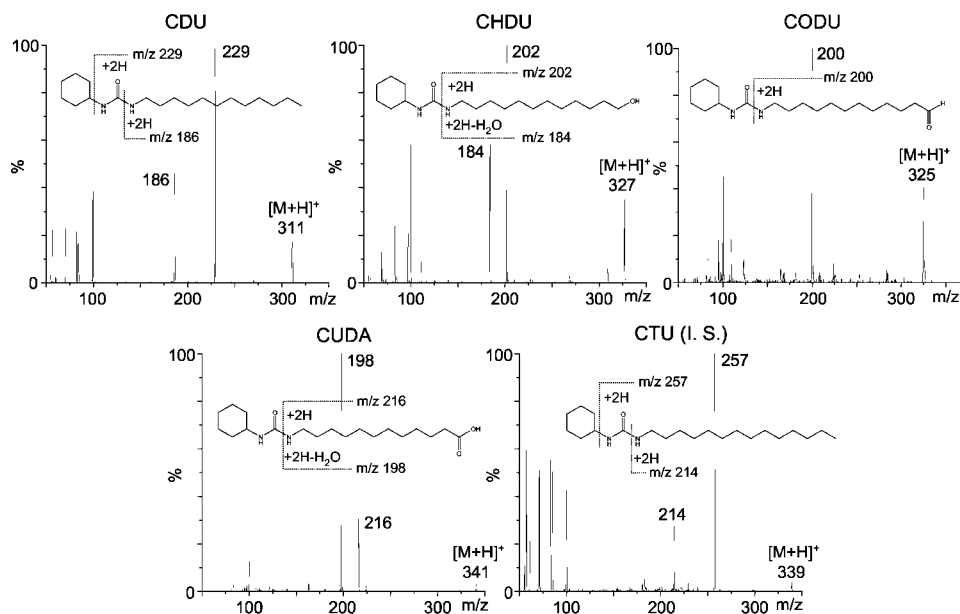

FIG. 1. *ESI tandem mass spectra of CDU, the primary CDU metabolites, and the internal standard (CTU).*

TABLE 1

Optimized ESI MS-MS parameters

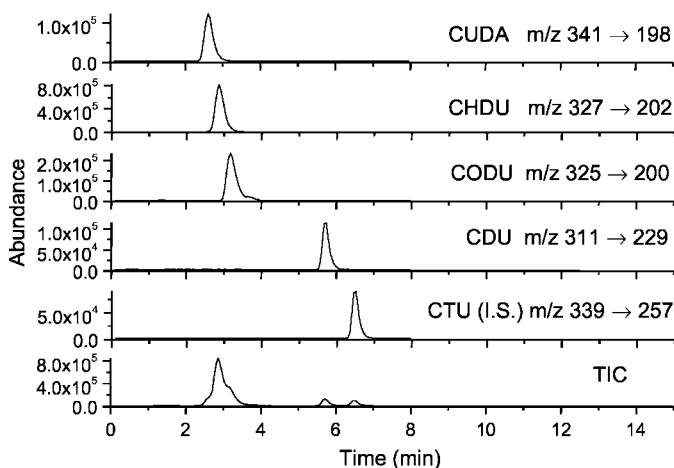| Analyte	Parent Ion [M + H]$^+$	Product Ion	Capillary Voltage	Cone Voltage	Collision Voltage
			kV	*V*	
CDU	311	229	1.0	80	27
CHDU	327	202	1.0	80	25
CODU	325	200	1.0	80	20
CUDA	341	198	1.0	85	32
CTU (I.S.)	339	257	1.0	100	30

I.S., internal standard.

FIG. 2. *Total ion chromatogram and MRM profiles of CDU and its metabolites.*

Separation conditions are described under *Material and Methods*. The retention times are as follows: CUDA, 2.6; CHDU, 2.9; CODU, 3.2; CDU, 5.7; and CTU, internal standard (I.S.), 6.5 min.

Metabolic Pathway Elucidation. The identified CDU metabolites suggested that the initial reaction leading to CHDU synthesis was a process that was most likely dependent on an enzyme or enzymes in the P450 4A family. To further implicate the P450 dependence, 1 μM CDU solution was incubated with rat microsomes for 10 min, purged with carbon monoxide for 1 min, and incubated for an additional 50 min at 37°C. The relative responses of CDU and CHDU against the internal standard (CTU) peak area were measured by LC/MS-MS. As shown in Fig. 5, the loss of CDU and the production of both CHDU and CUDA from CDU were significantly decreased upon microsome exposure to carbon monooxide. As further evidence of a P450 4A-mediated process, the CDU metabolite formation in noninduced and clofibrate-induced rat microsomes was compared (Fig. 6A). Not only was CDU metabolized to a greater extent in the clofibrate-induced microsomes, but the formation of CHDU, CODU, and CUDA was significantly ($P < 0.01$) higher, about 1.9-, 3.0-, and 2.8-fold, than that in noninduced microsomes. The effect of ABT on CDU metabolism was investigated (Fig. 6B). The microsomes were preincubated with 10 mM ABT for 10 min and further incubated for 20 min. The percentages of residual CDU increased with added ABT, whereas the percentages of CUDA formation significantly ($P < 0.05$) decreased with added ABT.

The transformation of the ω-hydroxylate to the terminal aldehyde moiety could be accomplished through either an NADPH-dependent P450-mediated mechanism, an NAD-dependent alcohol dehydrogenase-mediated mechanism, or perhaps both. To segregate these possibilities, rat microsomes were first preincubated with 1 μM CDU in the presence of a NADPH generating system for 40 min to produce a metabolite mixture. To evaluate the P450-related alcohol oxygenase component, this mixture was then enriched with additional rat micro-
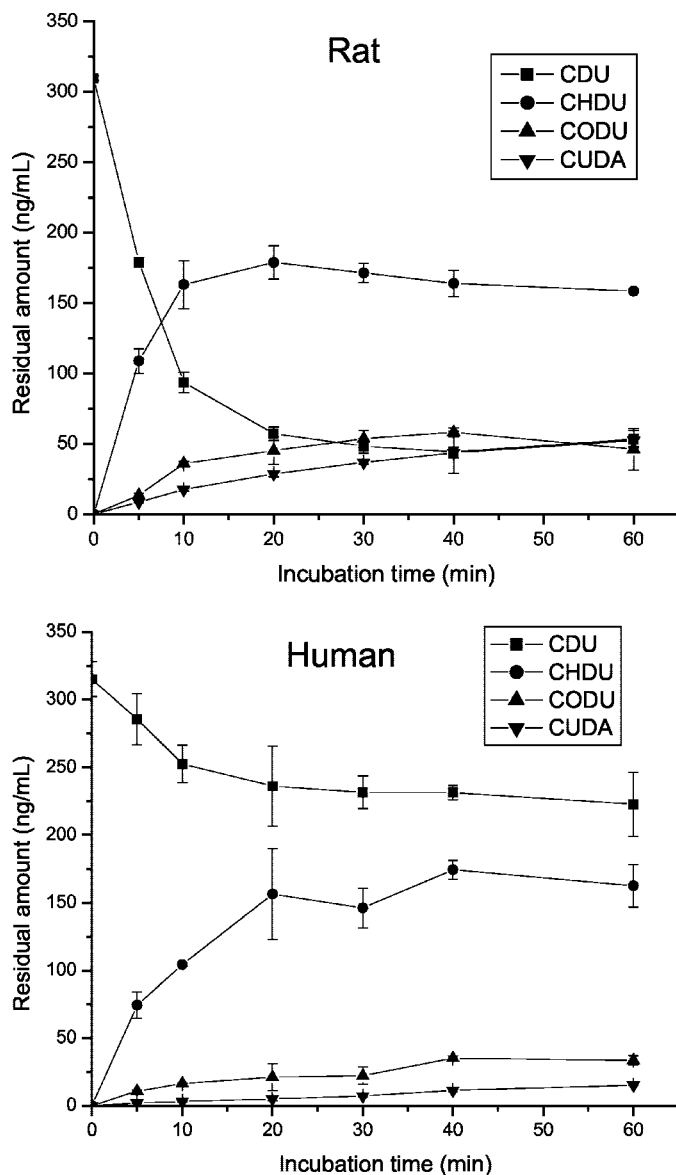

FIG. 3. *Time-dependent formation of CDU metabolites in rat and human hepatic microsomes.*

Microsomes were incubated with 1 μM CDU in the presence of a NADPH generating system. Data are expressed as means ± S.D. of triplicate experiments.

somes and a NADPH generating system, and incubated for 40 min. As shown in Fig. 7, coincubation with the NADPH generating system reduced CHDU concentrations and increased CUDA concentrations, whereas the trace levels of CDU remaining were unchanged. To evaluate the alcohol and aldehyde dehydrogenase-mediated components of CDU metabolism, a metabolite mixture was prepared as
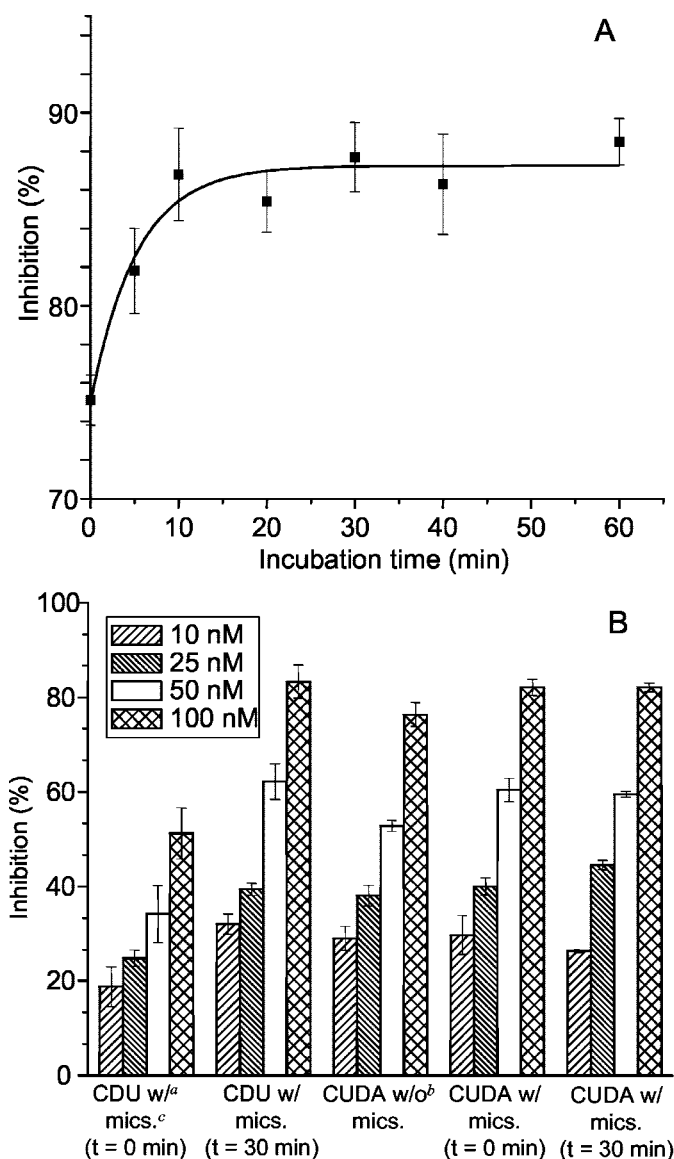
FIG. 4. *Effect of microsomes on sEH inhibition by CDU.*

After incubation in rat hepatic microsomes, 100 nM CDU was incubated in triplicate for 5 min in sodium phosphate buffer, pH 7.4, at 30°C with the recombinant enzyme (2 nM murine sEH). The time courses of sEH inhibition are shown in A. In B, the inhibition by 10 to 100 nM inhibitors was determined. *a*, w/, with; *b*, w/o, without; *c*, mics., microsomes.

FIG. 5. *Effect of carbon monoxide on the metabolism of CDU in rat hepatic microsomes.*

After 10 min of incubation with the NADPH generating system at 37°C in rat hepatic microsomes, the microsomes purged with carbon monoxide were further incubated for 50 min. The samples were analyzed by LC/MS-MS (see *Materials and Methods*). The response of each compound is expressed as the ratio of peak area against internal standard (CTU). Data are expressed as the means ± S.D. of triplicate experiments. *, $P < 0.05$, **, $P < 0.01$, significantly different from control.

tigated the transformation of a model sEH inhibitor (Morisseau et al., 2002), CDU, in rat and human hepatic microsomes.

Incubation of rat hepatic microsomes with CDU results in the formation of three major metabolites (Fig. 1). Since these compounds are nonvolatile and do not contain useful chromophores or fluorophores, analytical options for their detection and quantification are limited. However, using a highly specific and sensitive HPLC-tandem mass spectrometry system, we have developed a method for the simultaneous quantification of CDU and these metabolites. Analytical standards for the hydroxyl (CHDU) or oxo (CODU) compound metabolites could not be acquired for this study. However, upon collision-induced dissociation, both CUDA and these two metabolites produce primary fragments resulting from the loss of the aliphatic amine from the urea structure (Fig. 1). Therefore, to estimate the concentrations of these metabolites, the CUDA calibration curve was used as a pseudocalibration for CHDU and CODU. When this procedure was used to quantify residues in the time-dependent microsomal incubations experiments, the sum of the measured analytes at each time point corresponded to the initial CDU amount (Fig. 3). These results suggest that the use of CUDA calibration curves for estimating CHDU and CODU concentrations was valid and support the contention that the extraction recoveries of CHDU and CODU are similar to that of CUDA. A 30-mm reversed phase column was used to shorten analytical time, such that adequate separation of all analytes was achieved within 7 min using MRM mode detection. Using this method, we investigated the route and rate of CDU metabolism in rat hepatic microsomes.

Previously, we have reported that the metabolism of CDU in rat hepatic microsomes was rapid (Watanabe et al., 2001). To estimate the in vitro metabolic rate, we measured the kinetics of the NADPH-dependent metabolism of CDU to CHDU with rat hepatic microsomes. The calculated K_m (223 nM) and V_{max} (1.7 nmol/min/mg) for CDU suggest that this compound is an excellent substrate for cytochromes P450, most likely a CYP4A. Comparing the results to those reported by Amet et al. (1995) for 12-laurate hydoxylase activity (K_m

above and enriched with fresh rat microsomes and 2 mM NAD, and incubated for 40 min (Fig. 8). The addition of NAD significantly enhanced the transformation of CHDU to CUDA, doubling the responses of both CODU and CUDA.

Discussion

The soluble epoxide hydrolase is a novel pharmacological target with potential utility in the treatment of hypertension as well as renal and vascular inflammation (Imig et al., 2002). Di-substituted ureas have been identified as potent inhibitors of this enzyme, with some in vivo efficacy (Morisseau et al., 2002). Although little is known about the pharmacokinetics of these compounds, by understanding the dominant routes of metabolism, novel pharmacological agents can be designed to suppress these transformations and thereby optimize in vivo potency. To identify these routes of metabolism, we have inves-
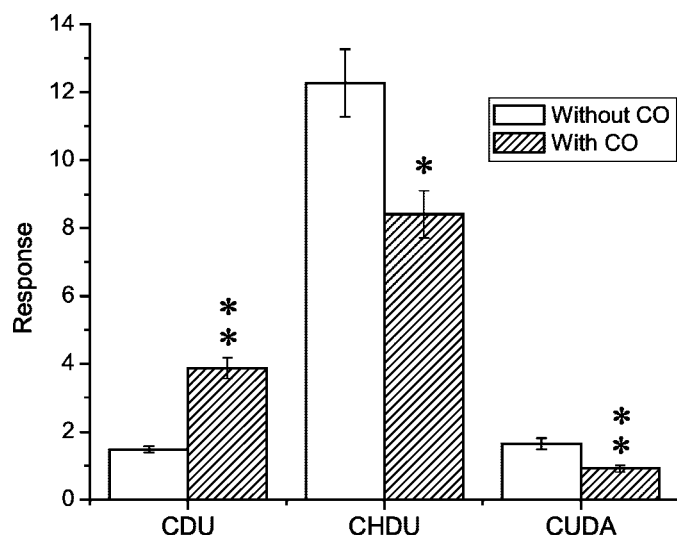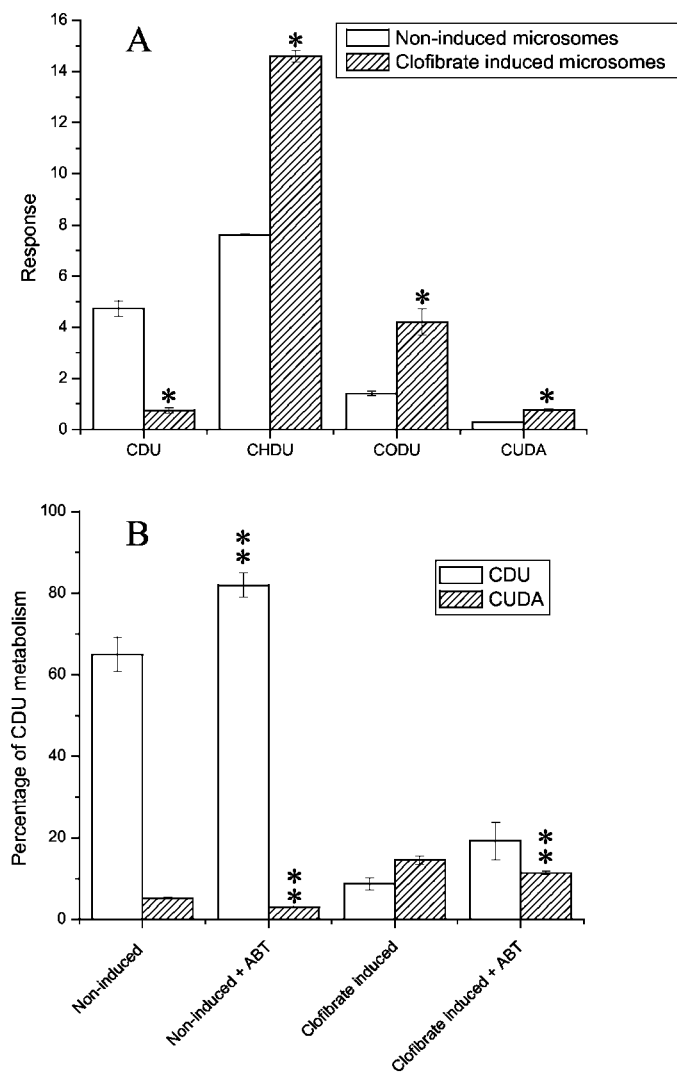
FIG. 6. *Effect of clofibrate induction on the metabolism of CDU in rat hepatic microsomes.*

A, microsomes were incubated for 20 min with 1 μM CDU in the presence of a NADPH generating system. In B, the microsomes were preincubated with 10 mM ABT for 10 min. Data are expressed as mean $\pm$ S.D. of triplicate experiments. *, $P < 0.01$, significantly different from control; **, $P < 0.05$, significantly different from control.

$= 13$ μM; $V_{max} = 2.1$ nmol/min/mg) suggests that CDU is at least a 40-fold better substrate for the rat ω-hydroxylase than lauric acid is for the human ω-hydroxylase.

When cytochrome P450 was inhibited by purging with carbon monooxide, the formation of the ω-hydroxylate of CDU was decreased ($P < 0.05$). Whereas carbon monoxide reduced CHDU formation by 20 to 30%, CUDA formation was reduced 45% (Fig. 5). This result suggests that carbon monoxide may inhibit the microsomal oxygenase or hydrogenase. The long alkyl chain (carbon = 12) of CDU may be metabolized by the CYP4A family (Nebert et al., 1985; Hardwick et al., 1987; Sharma et al., 1989; Okita et al., 2001). Indeed, lauric acid (dodecanoic acid) was the most efficiently hydroxylated (Adas et al., 1999), and the rank of catalytic activity was lauric > myristic > palmitic. We also found that the sEH inhibitor with a 10-carbon alkyl chain was also easily metabolized in rat hepatic microsomes (Watanabe et al., 2001). Although the ω- and ω-1-hydroxylic derivatives of CDU cannot be separated by our LC/MS-MS method (Fig. 2), we can clarify that the ω-hydroxylic deriv-
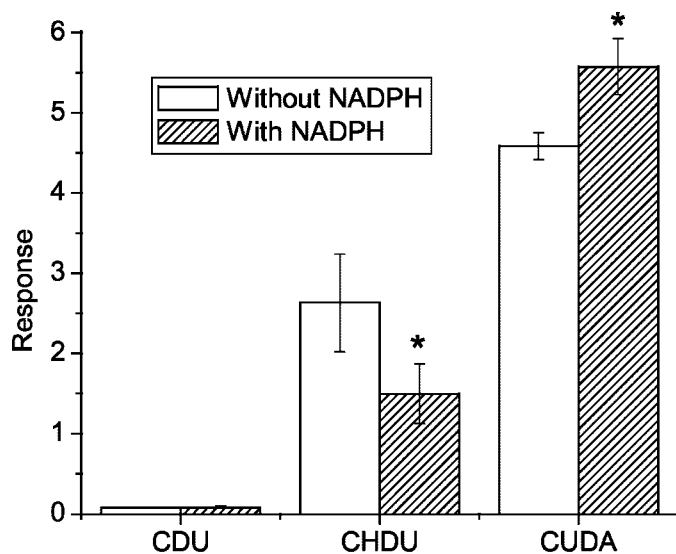

FIG. 7. *Effect of NADPH on the metabolism of CHDU in rat hepatic microsomes.*

After a 40-min incubation with the NADPH generating system at 37°C in rat hepatic microsomes, a 300-μl sample aliquot was mixed with 600 μl of microsomes and 100 μl of NADPH generating system and incubated for an additional 40 min at 37°C. The samples were analyzed by LC/MS-MS (see *Materials and Methods*). The response of each compound is expressed as the ratio of peak area against internal standard (CTU). Data are expressed as the means $\pm$ S.D. of triplicate experiments. $\star$, $P < 0.05$ significantly different from control.
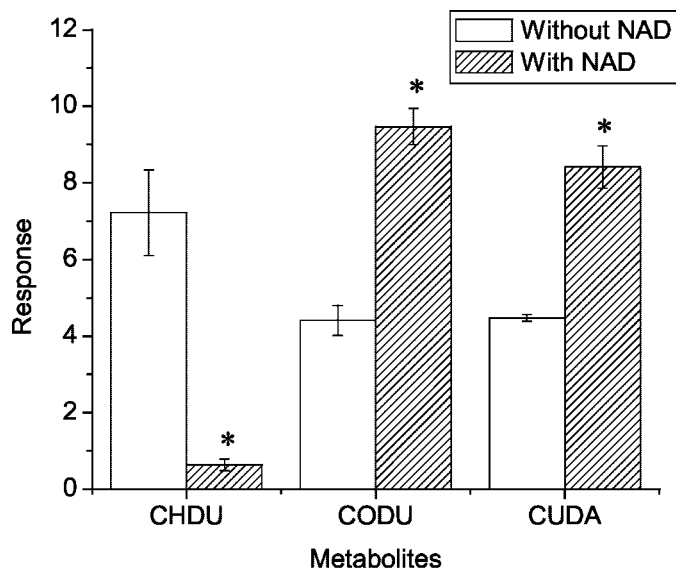

FIG. 8. *Effect of NAD on the metabolism of CUDA in rat hepatic microsomes.*

After a 40-min incubation with the NADPH generating system at 37°C in rat hepatic microsomes, a 300-μl sample aliquot was mixed with 600 μl of microsomes and 100 μl of 2 mM β-NAD, and incubated for an additional 40 min at 37°C. The samples were analyzed by LC-MS-MS (see *Materials and Methods*). The response of each compound is expressed as the ratio of peak area against internal standard (CTU). Data are expressed as the means $\pm$ S.D. of triplicate experiments. $\star$, $P < 0.01$, significantly different from control.

ative is the dominant hydroxylated metabolite from CDU in rat hepatic microsomes by use of a long reversed phase column (data not shown). As shown in Fig. 6A, the formation of CHDU in clofibrate-induced rat microsomes was 1.9-fold higher than that in noninduced microsomes. Moreover, we confirmed that the P450 4A1 activity, i.e., 12-laurate hydroxylase activity, of clofibrate-induced microsomes was 7-fold higher than that of noninduced microsomes. Together,

these results suggest that CDU was metabolized to CHDU by a cytochrome P450 in the 4A family. Moreover, the inhibition with ABT also supports our finding. As shown in Fig. 3, CDU was quickly metabolized to the ω-hydroxylate in rat hepatic microsomes, and was further metabolized to aldehydic (CODU) and carboxylic (CUDA) derivatives.

In human microsomes, the time-dependent formation profiles of CDU metabolites were similar to that of rat microsomes. However, only 30 to 40% formation of CODU and CUDA was observed, and the CDU profile was different from that of rat microsomes. These observations suggest that rat pharmacokinetic results may be weak predictors for human pharmacokinetics with respect to these aliphatic-containing compounds.

To confirm sEH inhibition by CDU after incubation with microsomes, the time course of sEH inhibition by CDU and CUDA was investigated (Fig. 4). Although ~70% of CDU was metabolized to CUDA and CHDU within 10 min of incubation (Fig. 3), sEH inhibition was increased by 10% (Fig. 4). In addition, CUDA was extremely stable in rat hepatic microsomes, with over 90% of CUDA still remaining after 60 min of incubation (data not shown). This result suggests that not only CUDA but also the ω-hydroxylic derivative (CHDU) is an excellent sEH inhibitor. These findings agree with the fact that sEH, the pharmacological target, can accept polar functionalities that are at a significant distance from the pharmacophore (Morisseau et al., 2002).

The described results have been summarized into a proposed metabolic pathway of CDU in rat hepatic microsomes (Fig. 9). We
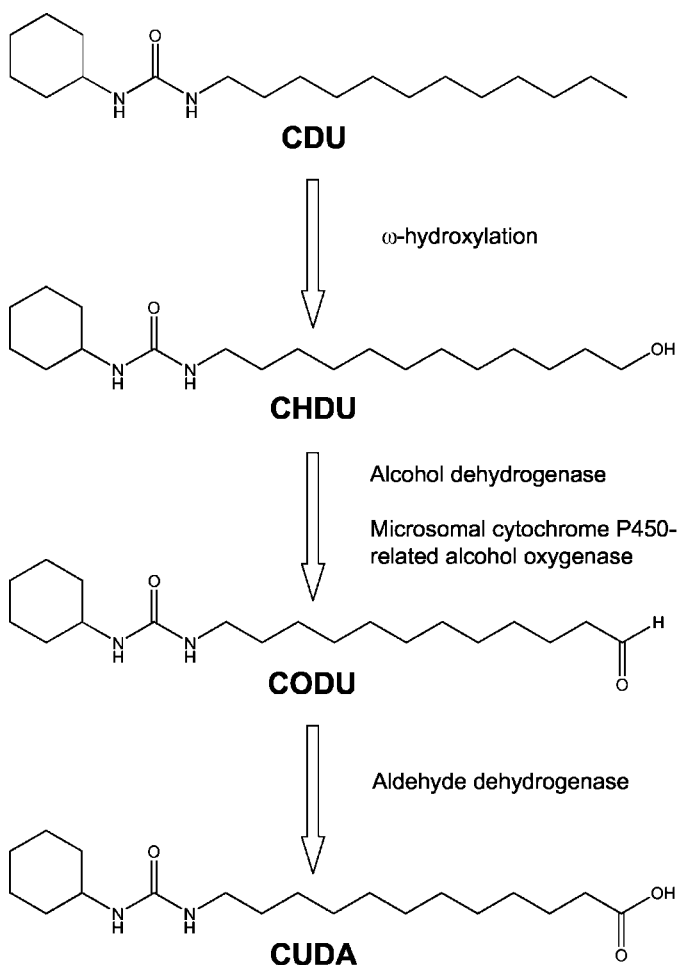

FIG. 9. *Proposed metabolic pathway of CDU in rat hepatic microsomes.*

designed two experiments to clarify our hypothesis of a metabolic pathway from hydroxylic derivative to carboxylic derivative (Figs. 7 and 8). The formation of aldehydic and carboxylic derivative was gradually increased with an increase in incubation time. On the other hand, the formation of hydroxy derivative was rapid, and the maximum concentration was reached at 20 min of incubation. As shown in Fig. 9, several enzymes are associated to act in this metabolic pathway, and CUDA may be generated by a two-step mechanism. When additional microsomes with NADPH generating system were added to rat microsomes to enhance microsomal cytochrome P450 activity, the hydroxy derivative was significantly decreased without additional depletion of CDU ($P < 0.05$) (Fig. 7). This finding suggests that metabolism from hydroxylic derivative to aldehydic derivative is partly catalyzed by microsomal cytochrome P450-related alcohol oxygenase. Furthermore, we added NAD as a dehydrogenase cofactor (Fig. 8). Consequently, 90% of the hydroxy derivative was metabolized to aldehydic and carboxylic derivatives, a significant enhancement ($P < 0.01$). From these results, we can indicate that the main metabolic pathway from hydroxylic to carboxylic derivative of CDU is catalyzed by alcohol dehydrogenase and aldehyde dehydrogenase. Indeed, the metabolic pathway of sameridine, which is an amide-type local anesthetic-analgesic agent with a hexyl side chain, is similar to this pathway (Sohlenius-Sternbeck et al., 2000). Also, Sinz et al. (1997) have reported that the alkyl side chain of a fatty acid anilide is metabolized via a similar pathway.

In conclusion, the results suggest that CDU, which has a long alkyl chain, is metabolized to CUDA by a multistep pathway that includes cytochrome P450 hydroxylases, alcohol dehydrogenase and microsomal cytochrome P450-related alcohol oxygenase, and aldehyde dehydrogenase (Tottmar et al., 1973; Koivula et al., 1975) (Fig. 9). We found that the activity of sEH was increased with incubation in rat hepatic microsomes, suggesting that at least some of the metabolites of CDU are themselves potent sEH inhibitors. The solubility of these metabolites was much better than that of CDU. These results suggest that the synthesis of ester derivatives of CUDA will likely yield potent sEH inhibitors with improved aqueous solubility. In addition, the presence at the ω-position of functions not transformed by P450 will decrease metabolism of sEH inhibition and increase their in vivo stability.

References

Adas F, Berthou F, Salaün JP, Dréano Y, and Amet Y (1999) Interspecies variations in fatty acid hydroxylations involving cytochromes P450 2E1 and 4A. *Toxicol Lett* **110:**43–55.

Amet Y, Berthou F, Baird S, Dreano Y, Bail JP, and Menez JF (1995) Validation of the (ω-1)-hydroxylation of lauric acid as an in vitro substrate probe for human liver CYP2E1. *Biochem Pharmacol* **50:**1775–1782.

Borhan B, Mebrahtu T, Nazarian S, Kurth MJ, and Hammock BD (1995) Improved radiolabeled substrates for soluble epoxide hydrolase. *Anal Biochem* **231:**188–200.

Bradford M (1976) A rapid and sensitive method for the quantitation of microgram quantities of protein utilizing the principle of protein-dye binding. *Anal Biochem* **72:**248–255.

Capdevila JH, Falck JR, and Harris RC (2000) Cytochrome P450 and arachidonic acid bioactivation: molecular and functional properties on the arachidonate monooxygenase. *J Lipid Res* **41:**163–181.

Chacos N, Capdevila J, Falck JR, Manna S, Martin-Wixtrom C, Gill SS, Hammock BD, and Estabrook RW (1983) The reaction of arachidonic acid epoxides (epoxyeicosatrienoic acids) with a cytosolic epoxide hydrolase. *Arch Biochem Biophys* **223:**639–648.

Dixon M (1972) The graphical determination of Km and Ki. *Biochem J* **129:**197–202.

Fang X, Kaduce TL, Weintraub NL, Harmon S, Teesch LM, Morisseau C, Thompson DA, Hammock BD, and Spector AA (2001) Pathways of epoxyeicosatrienoic acid metabolism in endothelial cells. Implications for the vascular effects of soluble epoxide hydrolase inhibition. *J Biol Chem* **276:**14867–14874.

Gibson GG, Orton TC, and Tamburini PP (1982) Cytochrome P-450 induction by clofibrate. Purification and properties of a hepatic cytochrome P-450 relatively specific for the 12- and 11-hydroxylation of dodecanoic acid (lauric acid). *Biochem J* **203:**161–168.

Gill SS and Hammock BD (1979) Hydration of *cis*- and *trans*-epoxymethyl stearates by the cytosolic epoxide hydrolase of mouse liver. *Biochem Biophys Res Commun* **89:**965–971.

Grant DF, Storms DH, and Hammock BD (1993) Molecular cloning and expression of murine liver soluble epoxide hydrolase. *J Biol Chem* **268:**17628–17633.

Guengerich FP (1982) Microsomal enzymes involved in toxicology—analysis and separation, in *Principles and Methods of Toxicology* (Hayes AW ed.) pp 609–637, Raven Press, New York.

Halarnkar PP, Wixtrom RN, Silva MH, and Hammock BD (1989) Catabolism of epoxide fatty

esters by the purified epoxide hydrolase from mouse and human liver. *Arch Biochem Biophys* **272:**226–236.

Hammock BD, Storms D, and Grant D (1997) Epoxide hydrolases, in *Comprehensive Toxicology* (Sipes I, McQueen C, and Gandolfi A eds) vol 3, pp 283–305, Pergamon, Oxford.

Hardwick JP, Song BJ, Huberman E, and Gonzalez FJ (1987) Isolation, complementary DNA sequence and regulation of rat hepatic lauric acid ω-hydroxylase (cytochrome P-450$_{LAW}$). *J Biol Chem* **262:**801–810.

Imig JD, Zhao X, Capdevila JH, Morisseau C, and Hammock BD (2002) Soluble epoxide hydrolase inhibition lowers arterial blood pressure in angiotensin II hypertension. *Hypertension* **39:**690–694.

Koivula T and Koivusalo M (1975) Different forms of rat liver aldehyde dehydrogenase and their subcellular distribution. *Biochim Biophys Acta* **397:**9–23.

Moghaddam MF, Grant DF, Cheek JM, Greene JF, Williamson KC, and Hammock BD (1997) Bioactivation of leukotoxins to their toxic diols by epoxide hydrolase. *Nat Med* **3:**562–566.

Morisseau C, Goodrow MH, Dowdy D, Zheng J, Greene JF, Sanborn JR, and Hammock BD (1999) Potent urea and carbamate inhibitors of soluble epoxide hydrolases. *Proc Natl Acad Sci USA* **96:**8849–8854.

Morisseau C, Goodrow MH, Newman JW, Wheelock CE, Dowdy DL, and Hammock BD (2002) Structural refinement of inhibitors of urea-based soluble epoxide hydrolases. *Biochem Pharmacol* **63:**1599–1608.

Nebert DW and Gonzalez FJ (1985) Cytochrome P450 gene expression and regulation. *Trends Pharmacol Sci* **6:**160–164.

Oesch F (1973) Mammalian epoxide hydrolases: inducible enzymes catalyzing the inactivation of carcinogenic and cytotoxic metabolites derived from aromatic and olefinic compounds. *Xenobiotica* **3:**305–340.

Okita RT and Okita JR (2001) Cytochrome P450 4A fatty acid omega hydroxylases. *Curr Drug Metab* **2:**265–281.

Orton TC and Parker GL (1982) The effect of hypolipidemic agents on the hepatic microsomal drug-metabolizing enzyme system of the rat. Induction of cytochrome(s) P-450 with specificity toward terminal hydroxylation of lauric acid. *Drug Metab Dispos* **10:**110–115.

Sharma RK, Doig MV, Lewis DF, and Gibson GG (1989) Role of hepatic and renal cytochrome P-450 IV A1 in the metabolism of lipid substrates. *Biochem Pharmacol* **38:**3621–3629.

Sinz MW, Black AE, Bjorge SM, Holmes A, Trivedi BK, and Woolf TF (1997) In vitro and in vivo disposition of 2,2-dimethyl-*n*-(2,4,6-trimethoxyphenyl) dodecanamide (CI-976). *Drug Metab Dispos* **25:**123–130.

Slim R, Hammock BD, Toborek M, Robertson LW, Newman JW, Morisseau CHP, Watkins BA, Saraswathi V, and Hennig B (2001) The role of methyl-linoleic acid epoxide and diol metabolites in the amplified toxicity of linoleic acid polychlorinated biphenyls to vascular endothelial cells. *Toxicol Appl Pharmacol* **171:**184–193.

Sohlenius-Sternbeck A-K, Chelpin HV, Orzechowski A, and Halldin MM (2000) Metabolism of sameridine to monocarboxylated products by hepatocytes isolated from the male rat. *Drug Metab Dispos* **28:**695–700.

Tottmar SOC, Peterson H, and Kiessling KH (1973) The subcellular distribution and properties of aldehyde dehydrogenase in rat liver. *Biochem J* **135:**577–586.

Watanabe T and Hammock BD (2001) Rapid determination of soluble epoxide hydrolase inhibitors in rat hepatic microsomes by high performance liquid chromatography with electrospray tandem mass spectrometry. *Anal Biochem* **299:**227–234.

Wixtrom RN and Hammock BD (1985) Membrane-bound and soluble-fraction epoxide hydrolases: methodological aspect, in *Biochemical Pharmacology and Toxicology* (Zakim D and Vessey DA, eds) vol 1, pp 1–93, John Wiley & Sons, Inc, New York.

Yu Z, Xu F, Huse LM, Morisseau C, Draper AJ, Newman JW, Parker C, Graham L, Engler M, Hammock BD, et al. (2000) Soluble epoxide hydrolase regulates hydrolysis of vasoactive epoxyeicosatrienoic acid. *Circ Res* **87:**992–998.

Zeldin DC, Wei S, Falck JR, Hammock BD, Snapper JR, and Capdevila JH (1995) Metabolism of epoxyeicosatrienoic acids by cytosolic epoxide hydrolase: substrate structure determinants of asymmetric catalysis. *Arch Biochem Biophys* **316:**443–451.

Zheng J, Plopper CG, Lakritz J, Storms DH, and Hammock BD (2001) Leukotoxin-diol: a putative mediator involved in acute respiratory distress syndrome. *Am J Respir Cell Mol Biol* **25:**434–438.